JOURNAL OF CATALYSIS 51, 314–325 (1978)

Infrared Studies of Carbon Monoxide and Hydrogen Adsorbed on Silica-Supported Iron and Cobalt Catalysts

M. J. HEAL, E. C. LEISEGANG, AND R. G. TORRINGTON

School of Chemistry, University of Cape Town, Rondebosch 7700, Cape, Republic of South Africa

Received November 22, 1976; revised October 3, 1977

A temperature-programmed infrared study of carbon monoxide and carbon monoxide–hydrogen mixtures adsorbed on silica-supported iron and cobalt catalysts was made. Bands observed at 2181 and 2169 cm^{-1} for carbon monoxide on cobalt and iron, respectively, were attributed to physical adsorption on oxide impurities. For cobalt a band observed in the range 2020 to 2060 cm^{-1} increased in frequency within this range as the CO pressure was increased. This change in frequency was pressure reversible. This has been interpreted in terms of the number of CO ligands bound to one cobalt atom. In the presence of iron a mixture of carbon monoxide and hydrogen gives rise to methane as well as to a small amount of ethane plus traces of propane. Preadsorption of hydrogen leads to formation of methane only. In the presence of cobalt, mixtures of carbon monoxide and hydrogen only give methane. A band attributed to linearly held carbon monoxide on cobalt has been correlated with methane formation. An intermediate complex formed between adsorbed carbon monoxide on cobalt and hydrogen, stable within the temperature range 125 to 195°C, has been inferred from the limited methane formation within this temperature range.

INTRODUCTION

This paper, which covers the adsorption of CO and H_2, either individually or as mixtures on iron and cobalt catalysts, is a continuation of earlier studies on nickel (*1*). Consequently, the objectives remain unaltered, viz., to investigate the effect of a regularly varying temperature on the adsorption and reactions of CO, either alone or with H_2 present, both in the gas phase and on the catalyst surface.

Infrared spectroscopy has not often been used to study the catalytic nature of cobalt. Gardner and Petrucci (*2*), from the spectra of CO on cobalt and other transition metals, postulated a relationship between the ligand's frequency and the number of valence electrons associated with it. Basila (*3*) observed infrared bands for CO on cobalt in the ranges 2179–2140 and 2091–2070 cm^{-1}, but assigned no structures to the species responsible for these absorptions. A more comprehensive study on the adsorption of CO on potassium-promoted and unpromoted Co/SiO_2 catalysts was given by Ferriera (*4*), from which the general conclusions reached on the interpretation of the spectra also applied to nickel (*4, 5*).

Other investigations were confined to the evaporated thin-film technique. Harrod *et al.* (*6*) observed very broad bands, attributable to adsorbed CO, on both iron and cobalt. The spectra did not change on evacuation, but on warming the maxima shifted to lower frequencies accompanied by a decrease in intensity.

The authors considered this to be due to

0021-9517/78/0513-0314$02.00/0

desorption of some CO, conversion to a less strongly absorbing state, or sintering of the metal. Similar conclusions were reached by Baker *et al.* (*7*). Bradshaw and Pritchard (*8*) recorded spectra of CO on thin cobalt films deposited at 113 K under ultrahigh vacuum and found these to be similar to spectra given by silica-supported cobalt. A band at 2040 cm^{-1} shifted to lower frequencies upon both warming and evacuation in contrast to earlier findings (*6*). But it is interesting to note that readsorption of CO did not bring back this high-frequency band.

Iron catalysts prepared in the laboratory are well known for their inability to form stable surface complexes with carbon monoxide (*4*). Not only do the thermodynamics of reactions of Fe, Ni, and Co predict (*9*) that ferric oxide is more difficult to reduce at high temperatures relative to nickel and cobalt oxides, but also the Fe–CO system has been found (*7, 10, 11*) to be very sensitive to small traces of oxygen. Traces of oxygen cause a low-frequency band at about 1960 cm^{-1} to disappear and to be replaced by one at a very much higher frequency. Adsorption of CO on ferric oxide of different reduction states, studied by Voroshilov *et al.* (*12*), gave rise to bands in the infrared spectrum at 2180, 2070, and 2020 cm^{-1} for CO adsorbed on Fe_2O_3, FeO, and Fe, respectively. The interaction of CO and H_2 on silica-supported iron at temperatures $>180°C$ gave three bands in the C–H stretching region which were assigned by Blyholder and Neff (*10*) to free methane. The infrared evidence was in accord with intermediates of the following types.

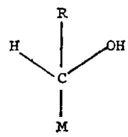

and

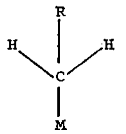

EXPERIMENTAL METHODS

The experimental methods used and the procedures adopted in this work are similar to those described elsewhere (*1*). First, the composition of reactant and product gases as a function of time, or as a function of time and temperature, were followed by means of a small Pyrex reactor connected to a vacuum line and to a 10-cm-path length infrared cell fitted with CaF_2 windows. The reactor contained up to 0.7 g of powdered material. Second, the infrared spectra of adsorbed species on pressed catalyst disc were studied in the frequency range 2300–1700 cm^{-1}. For these experiments the *in situ* infrared cell described earlier (*13*) was used. The temperature of both reactor and *in situ* cell could be raised smoothly to 400°C over a period of about 3 hr using a motor-driven variable autotransformer.

In the reactor experiments, measured amounts of CO and H_2 added either singly or as a mixture were admitted to the reactor and gas cell. The spectrum was scanned over the frequency range 4000–1000 cm^{-1} before and after the reactant gases were admitted at room temperature, and also after the reactor had reached 400°C. During the heating procedure the methane $\nu_3 Q$ branch at 3017.5 cm^{-1} was monitored continuously.

During the *in situ* cell experiments a background spectrum was recorded at room temperature. Gas was then admitted, and the spectrum was again recorded after a standing period of about 1 hr. On those occasions when the cell was evacuated prior to heating the spectrum was rerecorded. During heating, either the spectrum was scanned at half-hourly intervals, or given adsorbed species, termed A and B, were monitored at 1980 and 2169 and at 2020 and 2181 cm^{-1}, corresponding to iron and cobalt catalysts, respectively.

A Perkin–Elmer Model 180 double-beam infrared spectrometer was used, and the maximum slitwidth corresponded to a resolution of 2 cm^{-1}.

Material for use in the reactor was prepared by mixing silica with salt solu-

TABLE 1

Sample Composition and Preparation

(a) Reactor samples

Metal	Salt	Solvent[a] (ml)	Decomposition/ reduction temperature (°C)	Reduction time (hr)
5 wt% Fe	$Fe(NO_3)_3 \cdot 9H_2O$	H_2O (30 ml)	390–425	10–16
5 wt% Fe 0.1 wt% Cu	$Fe(NO_3)_3 \cdot 9H_2O$ $Cu(NO_3)_2 \cdot 3H_2O$	H_2O (30 ml)	400–440	12
5 wt% Fe	$FeOH \cdot (CH_3COO)_2$	Ethyl alcohol (90 ml)	410–435	12
5 wt% Co	$Co(NO_3)_2 \cdot 6H_2O$	Acetone/water (50 ml/1 ml)	385–410	11–12

(b) *In situ* samples

Metal	Salt	Concentration of salt in solution (%, w/v)	Decomposition/ reduction temperature (°C)	Reduction time (hr)
4.5–5.0 wt% Fe	$Fe(NO_3)_3 \cdot 9H_2O$ $Cu(NO_3)_2 \cdot 3H_2O$	45 0.27	390–465	6–24
5.5–6.0 wt% Co	$Co(NO_3)_2 \cdot 6H_2O$ Acetone/water (50 ml/8 ml)	50	385–430	12–22

[a] Per 10 g of material (salt + SiO_2).

tions of iron and cobalt (either the nitrate or acetate), drying, and grinding into fine powders. Each salt was then decomposed and reduced in the reactor in the usual way. All catalysts contained 5 wt% metal. To facilitate reduction 0.1 wt% Cu was added to one of the iron catalysts. Samples for use in the *in situ* cell were prepared by first pressing a silica disc 25 mm in diameter and 0.2–0.3 mm thick. This was then simply dipped into a salt solution of appropriate concentration (designed to yield 4–6 wt% metal), dried, decomposed, and reduced *in situ*. Decomposition/reduction times and temperatures were more severe for iron than for cobalt catalysts. These experimental conditions are summarized in Table 1. For iron higher temperatures and longer reduction periods ensured sufficiently well-reduced samples. Long reduction peroids were found to be unnecessary for reactor samples because of their physical form. All samples were allowed to decompose to their oxides over a period of 4 hr.

RESULTS

1. *Cobalt*

(*a*) *Reactor experiments.* The four procedures, CO–H_2–ΔH, CO/H_2–ΔH, H_2–CO–ΔH, and CO–ΔH, were applied in turn to the cobalt catalysts. Here the order of addition of reactant gases was of prime importance, and the above notation, described earlier (*1*), will be used in the presentation of these results and those of iron. For example, the notation CO–H_2–ΔH means that the catalyst was subjected to carbon monoxide, hydrogen, and heating in that order. The results were as follows.

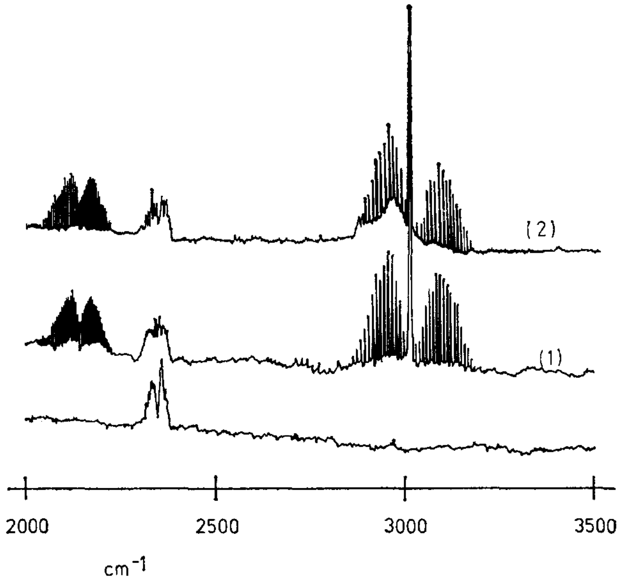

FIG. 1. Spectra of products at 400°C from (1) CO followed by H_2 adsorbed on Co/SiO_2 and (2) CO and H_2 adsorbed on Fe/Cu/SiO_2, with background offset.

(i) In contrast to nickel (*1*), which readily formed $Ni(CO)_4$ on preadsorption of CO at room temperatures, no gaseous carbonyl was detected at any stage.

(ii) Carbon dioxide, estimated spectroscopically from the intensity of the 2345 cm^{-1} fundamental, was the only product formed on applying procedure CO–ΔH. The amount produced decreased on aging and/or sintering of the catalyst.

(iii) Methane was the main product of all experiments in which CO and H_2 were present. Considerable amounts were produced, comparing well with those observed for Ni (*1*) under the same conditions. This is shown in Fig. 1 for the procedure CO–H_2–ΔH. CH_4 was first detected in the temperature range 195–215°C, slightly higher than that for Ni (190°C). No other hydrocarbons, either saturated or unsaturated, were observed by infrared spectroscopy and only trace amounts of ethane were detected by mass spectroscopy when the procedure CO–H_2–ΔH was applied.

(iv) A CO/H_2 mixture admitted at various fixed catalyst temperatures revealed that, over a 2-hr period, CH_4 was produced (although in limited quantities) well below 195°C. It can be seen from Fig. 2 that only trace amounts would be formed in the range 100–130°C and none would be formed below this range.

(*b*) *In situ cell experiments.* In contrast to nickel (*1*), cobalt catalyst disc rapidly became inactive on heating. Also relatively high CO pressures (40–50 Torr) were required in order to observe infrared absorption bands of medium intensity.

(i) The spectrum of CO chemisorbed on cobalt at room temperature is shown in Fig. 3. A narrow band (band B) was observed at 2181 ± 1 cm^{-1} together with a broad, medium band (band A) having maxima within the ranges 2062–2055 and 2037–2032 cm^{-1}. On evacuation (10 min) band B almost disappeared and band A narrowed and showed only one maximum shifted to the range 2027–2022 cm^{-1} (Fig. 3). On reintroduction of CO the original spectrum was restored. Continued cycles of evacuation and readmission of CO showed the adsorption reactions to be reversible. This reversibility phenomenon has not been observed before (*8*). Pro-

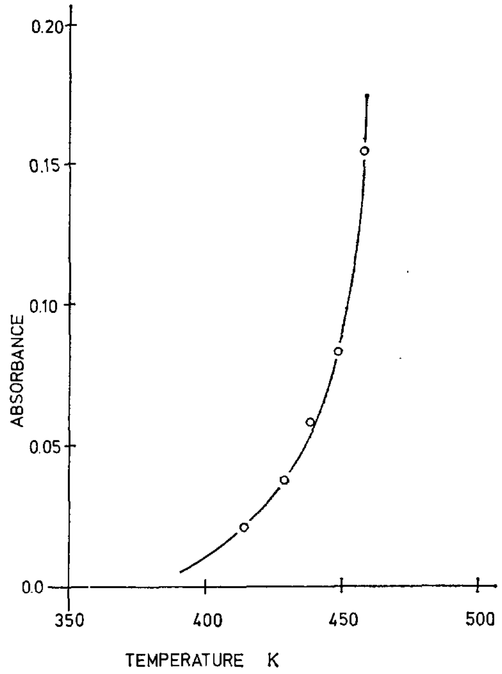

FIG. 2. Plot of absorbance as a function of temperature at 3017.5 cm^{-1} due to CH_4 resulting from adsorbed CO and H_2 on Co/SiO_2 over a 2-hr period.

longed evacuation caused no further significant change in the appearance of band A.

(ii) The effect on the spectra of varying the CO pressure is shown in Fig. 4. Band B increased in intensity with pressure reaching a maximum at about 55 Torr. Band A also increased with pressure, but its shape changed as follows. At low pressures (<10 Torr) it was broad with a flat top centered at 2040 cm^{-1}. At medium pressures (10–30 Torr) two maxima were observed of almost equal intensity at 2030 and 2055–2050 cm^{-1}, respectively. At high pressures (>30 Torr) the high-frequency maximum predominated and moved to 2060 cm^{-1}; the low-frequency maximum appeared as a shoulder at 2034 cm^{-1}.

(iii) The effect of heating was investigated both after evacuation and with excess H_2 present. Band A was monitored at 2020 cm^{-1} while the catalyst was heated slowly. Plots of the change in absorbance with temperature are shown in Fig. 5. The intensity of band A decreased linearly with temperature over the range 115–190°C for the evacuated system. With H_2 present the intensity decreased rapidly over the range 125–215°C, by which time band A had completely disappeared. Clearly the presence of H_2 affects the rate of disappearance of band A at elevated temperatures. In contrast to the findings for Ni (*1*), it is interesting to note that the lower temperature limits did not coincide with CH_4 formation (see Reactor Experiments, Section 1a) under similar experimental conditions.

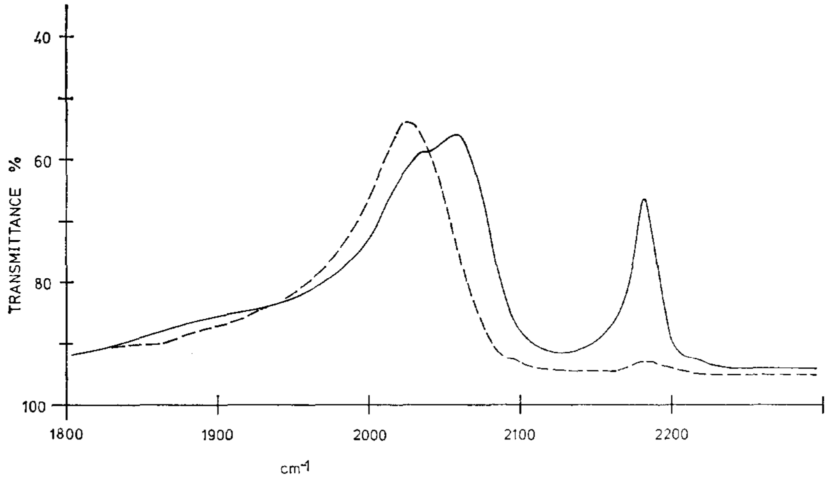

FIG. 3. Effect of evacuation on the spectrum of CO adsorbed on Co/SiO_2: (——) before evacuation; (- - - -) after evacuation.

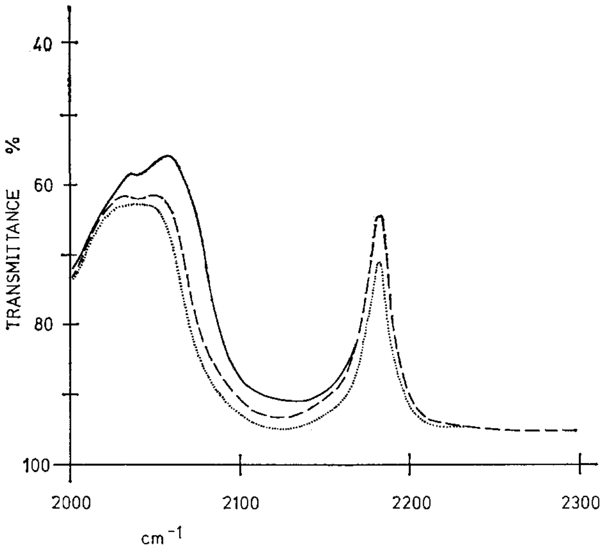

FIG. 4. Effect on the spectra of varying CO pressure on Co/SiO_2: (····) < 10 Torr; (- - - -) 10–30 Torr; (——) > 30 Torr.

(iv) The effect of H_2 on band A at 2022 cm^{-1} is shown in Fig. 6. All three spectra are shown for comparison purposes, i.e., CO adsorption before and after evacuation and CO_{ads} plus H_2. Thus the addition of H_2 caused band A to decrease in intensity and exhibit a high-frequency hump. In one experiment only the maximum of band A shifted to 2028 cm^{-1} on the admission of H_2 to the evacuated cell. This was not reproduced.

2. Iron

(*a*) *Reactor experiments.* Once again the four procedures CO–H_2–ΔH, CO/H_2–ΔH, H_2–CO–ΔH, and CO–ΔH, were applied in turn to each of the iron catalysts, Types Fe I, II, and III, which contained 5 wt% Fe prepared from the nitrate, 5 wt% Fe plus 0.1 wt% Cu prepared from their nitrates, and 5 wt% Fe prepared from the acetate, respectively. The results were as follows.

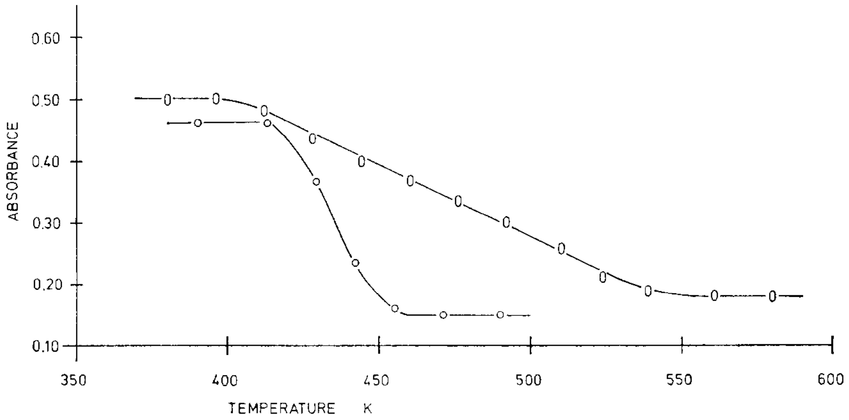

FIG. 5. Plot of absorbance as a function of temperature at 2020 cm^{-1}: (O) for CO alone on Co/SiO_2; (o) for CO_{ads} followed by H_2 on Co/SiO_2.

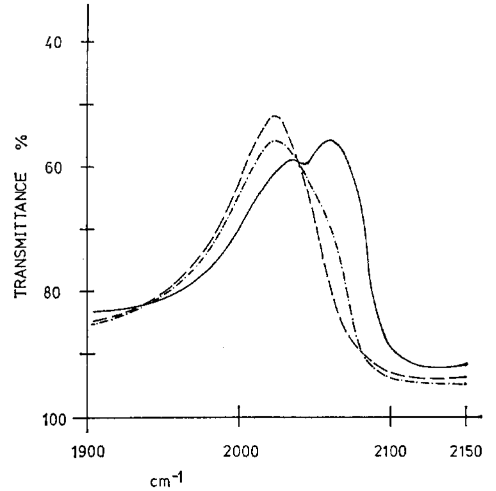

FIG. 6. Effect of H_2 on band A for CO adsorbed on Co/SiO_2: (——) CO alone before evacuation; (– – –) CO alone after evacuation; (–·–·) on addition of H_2).

(i) The interaction of CO and H_2 on all catalyst types, at high temperatures, formed methane as the chief product. However, methane was initially detected at much higher temperatures than those observed for either Ni or Co. These were (a) 200–220°C for a freshly reduced Fe sample and (b) 220–250°C for aged/sintered material.

(ii) For procedures CO–H_2–ΔH and CO/H_2–ΔH, when catalysts Fe II and III were used, small amounts of higher hydrocarbons were detected in terms of broad, very weak infrared absorptions at 2970 and 2880 cm^{-1}, characteristic of stretching vibrations of methyl groups. Mass spectrometric analysis confirmed the presence of small amounts of ethane and trace amounts of propane. A typical spectrum, recorded when the reactor had reached 400°C, is given by Fig. 1. On the other hand, methane was the only reaction product with the less active Fe I catalysts and also when procedure H_2–CO–ΔH was employed for all catalyst types.

(iii) The order of catalytic activity with respect to methane production, as measured in terms of the relative amounts of CH_4 formed, using freshly prepared samples, was found to be Fe II > Fe III > Fe I.

(iv) Usually no products were detected when the procedure CO–ΔH was applied except that, occasionally, a small increase in intensity of the CO_2 fundamental was observed at 2345 cm^{-1}.

(*b*) *In situ cell experiments.* Iron catalyst disc were found to be even less active than cobalt disc and once again relatively high CO pressures were necessary to produce significant absorption bands. The copper-promoted iron catalysts displayed

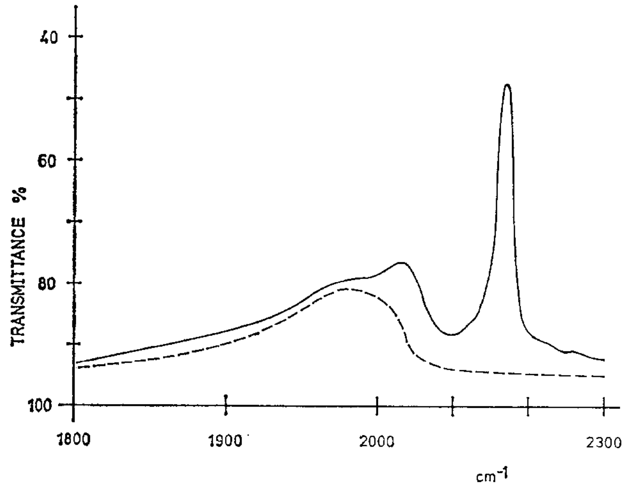

FIG. 7. Effect of evacuation on the spectrum for CO (41 Torr) adsorbed on $Fe/Cu/SiO_2$ reduced for >20 hr at 450°C: (——) before evacuation; (– – –) after evacuation.

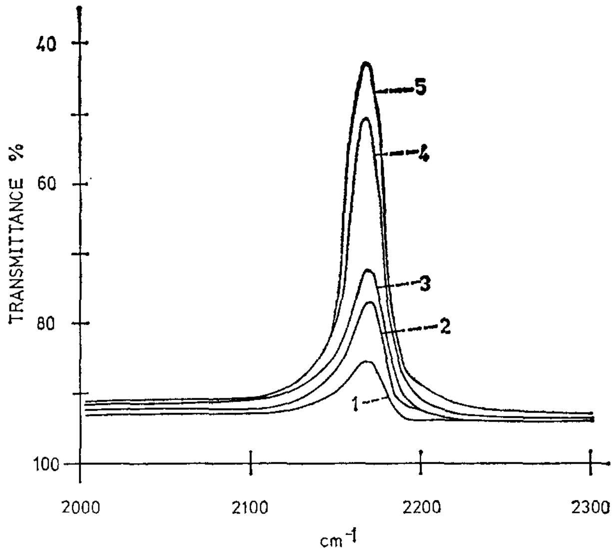

Fig. 8. Effect of CO pressure on band B at 2169 cm^{-1} for CO on Fe/Cu/SiO$_2$: (1) >1 Torr; (2) 5–6 Torr; (3) 19 Torr, reduced at 410°C. (4) 20 Torr; (5) 46 Torr, reduced at 450°C.

the greatest activity and therefore only the results obtained using these will be reported.

The spectrum of CO chemisorbed on iron is given in Fig. 7. A sharp band of medium intensity (band B) was observed at 2169 ± 1 cm^{-1} together with a very broad weak band (band A) having its maximum in the range 2030–2040 cm^{-1}. Band A showed a broad inflection at about 1980 cm^{-1} and had a low-frequency tail. Evacuation caused band B to disappear (cf. CO on cobalt) while A shifted to lower frequencies and decreased slightly in intensity. The final maximum of band A shifted to the range 1970–1980 cm^{-1} (Fig. 8). Band A was not observed when the catalyst had been reduced for shorter periods and at lower temperatures than stated earlier.

Band A was monitored at 1980 cm^{-1} while the catalyst was heated slowly and its intensity was found to decrease within the temperature range 100–140°C. Unfortunately, at temperatures > 200°C the "background" shift, similar to that found with nickel (*1*), masked any further observations. However, it was clear that at 200°C band A had decreased by approximately only half of its original intensity.

Regrettably, all the iron catalysts lost their activity very rapidly, and this limitation together with the very broad nature of band A inhibited detailed investigations.

The weakly held CO species giving rise to band B was also monitored at 2169 cm^{-1} during heating. Its intensity was found to decrease rapidly over the temperature range 25–180°C, with a marked increase in the rate of disappearance at temperatures >70°C. Band B at 2181 cm^{-1} for CO on cobalt gave similar results.

Finally, band B was observed to increase in intensity with an increase in the CO pressure. Figure 8 shows this pressure effect clearly. It is interesting to note that the higher reduction temperature, ~450°C, compared with 400°C (see plots 3 and 4), enhanced the adsorption of the CO species giving rise to band B.

DISCUSSION

The reversible shift observed in the frequency of the infrared bands for carbon monoxide adsorbed on cobalt, when the carbon monoxide pressure was varied, could be interpreted in the following manner.

The generally accepted explanation of the M–C bond of the M–C–O system is based on a molecular orbital model of the CO molecule. A C → M σ bond would be ineffective, being opposed by electrostatic repulsions arising from electron transfer. An M → C π bond would be similarly ineffective. However, taken together, the two electron transfers act in opposite directions and tend to cancel; relatively strong synergetic bonding results. The M → C component arises from the availability of *d*-electron density from the metal which occupies an empty CO antibonding orbital. Thus as the M–C bond strength increases, through greater availability of *d*-electron density, the C–O bond strength diminishes as shown by lower C–O vibration frequencies.

Previous interpretations (*4, 14–17*) of the infrared spectra of CO adsorbed on metals have associated the higher vibration frequencies with low *d*-density (high coordination number) crystal face sites and the lower frequencies with higher *d*-density (low coordination number) corner and/or edge sites of the metallic crystal.

The explanation given above is not very convincing when applied to our observations. These observations can be represented as follows:

$$2060(\mathrm{A}_z) + 2034(\mathrm{A}_y) \underset{\text{excess CO}}{\overset{\text{evacuation}}{\rightleftharpoons}} 2022(\mathrm{A}_x).$$

Band A changes reversibly from a single band (A_x) occurring at 2022 cm^{-1} in the evacuated system to a doublet having maxima at 2060 (A_z) and 2034 cm^{-1} (A_y) in the presence of excess carbon monoxide. If the frequency shift is due to rearrangement from plane sites to corner/edge sites when the system is evacuated it could be expected that the A_x band would be relatively weak because crystal planes have a comparatively much larger capacity than do corners/edges. In addition, when excess carbon monoxide is present the band at 2022 cm^{-1} should still be seen, as the addition of carbon monoxide should not cause desorption from more active sites (corners/edges). In view of the above a possible alternative explanation could be that the multiplicity and frequencies of the bands observed are due to the number of carbon monoxide ligands attached to a single cobalt atom. The shape of the band, however, could be dependent on factors such as ligand–ligand interaction, metal to metal distances, and the nature of the adsorption sites, e.g., planes, corners, and edges.

Thus for CO on cobalt, the bands found above 2000 cm^{-1} are assigned to the species $\mathrm{M(CO)}_z$, $\mathrm{M(CO)}_y$, and $\mathrm{M(CO)}_x$, corresponding to the bands A_z, A_y, and A_x, respectively, where $z > y > x \geqslant 1$, and for which the M–C bond strengths are in the order of $\mathrm{M(CO)}_x > \mathrm{M(CO)}_y > \mathrm{M(CO)}_z$. Were lower frequency bands assigned to bridged carbonyl structures to be observed they would follow the same pattern in that the lower frequency would correlate with the smaller CO:metal ratio. It may be possible to extend this interpretation to the infrared spectra of CO adsorbed on other metals such as nickel (*1*). Hence, band B (for CO on nickel) found at either 2080 (on CO preadsorption) or 2074 cm^{-1} (on H_2 preadsorption or on treatment with a $\mathrm{CO/H}_2$ mixture), can be ascribed to coadsorbed species having the structures $\mathrm{Ni(CO)}_x$ and $\mathrm{H}_z\mathrm{Ni(CO)}_y$, respectively, where $4 > x > y \geqslant 1$ and $z \geqslant 1$.

Within a system $\mathrm{M(CO)}_n$, any change in the value of n can be described as an "internal" one which would cause a considerable influence on the M–C and C–O bonds, because as n increases the *d* density per CO decreases. On the other hand, it is possible that "external" forces such as ligand–ligand interactions, dependent upon metal to metal distances and the nature of the adsorption sites, would have far less influence on the bond strengths. The position of infrared absorption bands depends solely on the C–O bond strength which, in turn, is mainly influenced by the M–C bond strength. This is the chief argument by which band frequency positions and observed band shifts can be assigned to changes in the value of n. For example, the influence shown by the CO:metal ratios 1:2 and 1:1 (bridged and linear species, respectively) has frequently been demonstrated by the large differences in their band positions. The shapes of infrared bands are due to the weaker "external" forces which, as a result of the large number of forces of this nature, are usually broad in appearance. Evidence in favor of this interpretation would be the following

(i) The reversible frequency shift suggested that a reaction had occurred according to the equation:

$$\mathrm{M(CO)}_z + \mathrm{M(CO)}_y \underset{\text{excess CO}}{\overset{\text{evacuation}}{\rightleftharpoons}} \mathrm{M(CO)}_x.$$

A similar reversibility was observed by Soma-Noto and Sachtler (*18*) for CO on Pd and Pd–Ag alloys.

(ii) The effect on band A of varying the CO pressure (Fig. 4) exhibited the expected equilibria:

$$\mathrm{M(CO)}_z \rightleftharpoons \mathrm{M(CO)}_y \rightleftharpoons \mathrm{M(CO)}_x.$$

(iii) The development of the hump on the high-frequency side of band A upon the addition of H_2 after CO further confirms the hypothesis that several ligands chemisorb on the same metal site.

In $H_yM(CO)_x$, where $y \geqslant 1$, the hydrogen competes for *d*-electron density and so weakens the M–C and strengthens the C–O bonding that a shift to higher CO infrared frequencies is observed. The extent of the shift would depend on two factors: (a) the ability of hydrogen to accept *d* electrons from the metal and thereby establish a chemisorbed M–H species; and (b) the relative proportions of *d*-electron density distributed between the M–H and M–C bonds within an H–M–CO species. Dalmon *et al.* (*19*) reported that hydrogen was more strongly adsorbed on nickel than on cobalt and this is confirmed by the present work on cobalt in comparison with previous findings (*1*) for nickel.

(iv) When the catalyst was heated slowly, while the spectrum was scanned continuously over the range 2300–1700 cm^{-1}, bands A_z and A_y decreased in intensity and were replaced by band A_x which increased in intensity. This result suggests a decrease in the value of n, until probably a value of 1 is obtained.

Despite the difficulty in the attainment of well-reduced active iron catalyst, the reactor experiments clearly demonstrated the tendency of this catalyst to promote the formation of longer chain hydrocarbons. Kölbel and Tillmetz (*20*) observed a special catalytic activity for chain propagation on Fe (111) surface clusters which was considered to proceed via an oxygenated species. A similar mechanism was proposed for cobalt, but the authors stated that the higher stability and strongly marked enolic behavior of the iron complex relative to the cobalt complex was responsible for the production of longer chain hydrocarbons. A different reaction mechanism was proposed for nickel which was not conducive toward chain propagation. The observed activity of all three metals, shown by infrared and mass spectrometric analysis of the products, here and previously (*1*), supported the findings of Kölbel and Tillmetz (*20*).

Allied to this was the interesting phenomenon observed when H_2 was preadsorbed on iron catalysts resulting in CH_4 being the only product detected. It seems likely that either hydrogen blocks those sites which favor the formation of higher hydrocarbons, or on coadsorption with CO a new intermediate complex is formed which itself has an inhibiting effect.

The sharp bands (b) at 2169 and 2181 cm^{-1} for CO on Fe and Co, respectively, were attributed in part to very weakly held chemisorbed CO, with perhaps some CO existing in a physisorbed state. The species were considered to be adsorbed onto the oxide impurities in agreement with the findings of Voroshilov *et al.* (*12*). On the other hand, band A at 2030 cm^{-1}, for CO on Fe, was more strongly held and was therefore assigned solely to chemisorbed CO having a linear structure.

Strong evidence was provided to show that linear CO species on cobalt were involved in the methane formation reaction mechanism which was similar to that proved for nickel catalysts (*1*). The rapid decrease in absorbance of band A over the temperature range 125–215°C (Fig. 5) for systems containing both CO and excess H_2 and the absence of such a decrease for those containing only CO confirmed that the species giving rise to band A was involved in methane formation.

The low-temperature range (125–215°C) observed for systems containing both H_2 and CO did not coincide with the methane formation temperature of 195°C under similar experimental conditions. That methane could be formed below the temperature range 195–215°C (see Fig. 2) simply demonstrates that its formation is dependent on both time and temperature. Therefore, it appears that, within the range 125–215°C, an intermediate complex was formed between the adsorbed CO and H_2 which does not absorb in the frequency range 2300–1700 cm^{-1}. The complex may well have been of an enolic nature, i.e., H–C(M)–OH, as reported by Balaji Gupta *et al.* (*21*) and later by Farrauto (*22*). Assuming this to be the case the mechanism of methane formation could be represented, providing thermal programming conditions are used, as follows.

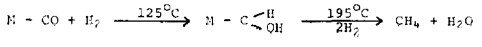

$$M - CO + H_2 \xrightarrow{125^\circ C} M - C{\scriptsize\begin{matrix}H\\OH\end{matrix}} \xrightarrow[2H_2]{195^\circ C} CH_4 + H_2O$$

These findings indicate that further progress is now possible because the above data provide the experimental parameters within which the intermediate may be studied. The structure and role of the intermediate in the reaction mechanism could then be determined more accurately.

On the other hand band B at 2030 cm^{-1} for CO/H_2 on Ni (*1*) decreased in intensity at a temperature which did coincide with the methane formation temperature of >190°C. Either the intermediate complex formed on nickel was less stable, or the rate-determining step in the mechanism was the formation of the intermediate and not the formation of CH_4.

REFERENCES

1. Heal, M. J., Leisegang, E. C., and Torrington, R. G., *J. Catal.* **42**, 10 (1976).

2. Gardner, R. A., and Petrucci, R. H., *J. Amer. Chem. Soc.* **82**, 5051 (1960).

3. Basila, M. R., *Appl. Spectrosc. Rev.* 1, 289 (1968).

4. Ferreira, L. C., Ph.D. Thesis, University of Cape Town, Cape Town, Republic of South Africa, 1970.

5. Ferreira, L. C., and Leisegang, E. C., *J. S. Afr. Chem. Inst.* **23**, 136 (1970).

6. Harrod, J. F., Roberts, R. W., and Rissman, E. F., *J. Phys. Chem.* **71**, 343 (1967).

7. Baker, F. S., Bradshaw, A. M., and Pritchard, J., *Surface Sci.* **12**, 426 (1968).

8. Bradshaw, A. M., and Pritchard, J., *Proc. Roy. Soc. Ser. A* **316**, 1525, 169 (1970).

9. Emmett, P. H., "Catalysis," Vol. 4. Van Nostrand Reinhold, New York, 1956.

10. Blyholder, G., and Neff, L. D., *J. Phys. Chem.* **66**, 1464 (1962).

11. Eischens, R. P., and Pliskin, W. A., *Advan. Catal.* **10**, 1 (1958).

12. Voroshilov, T. G., Lunev, N. K., Roev, L. M., and Rusov, M. T., *Dopov. Akad. Nauk Ukr. RSR Ser. B* **4**, 319 (1975).

13. Heal, M. J., Leisegang, E. C., and Torrington, R. G., *J. Sci. Instrum.* **7**, 352 (1974).

14. Yates, J. C., and Garland, C. W., *J. Phys. Chem.* **65**, 617 (1961).

15. Little, L. H., "Infrared Spectra of Adsorbed Species." Academic Press, London, 1966.

16. Hair, M. L., "Infrared Spectroscopy in Surface Chemistry." Marcel Dekker, New York, 1967.

17. Blyholder, G., *J. Phys. Chem.* **68**, 2772 (1964).

18. Soma-Noto, Y., and Sachtler, W. M. H., *J. Catal.* **32**, 315 (1974).

19. Dalmon, J. A., Martin, G. A., and Imelik, B., *Colloq. Int. Centre Nat. Rech. Sci.*, 593 (1971).

20. Kölbel, H., and Tillmetz, K. D., *J. Catal.* **34**, 307 (1974).

21. Balaji Gupta, R., Viswanathan, B., and Sastri, M. V. C., *J. Catal.* **26**, 212 (1972).

22. Farrauto, R. J., *J. Catal.* **41**, 482 (1976).